

## Optimal Targeted Lockdowns in a Multigroup SIR Model<sup>†</sup>

By DARON ACEMOGLU, VICTOR CHERNOZHUKOV,  
IVÁN WERNING, AND MICHAEL D. WHINSTON\*

*We study targeted lockdowns in a multigroup SIR model where infection, hospitalization, and fatality rates vary between groups—in particular between the “young,” the “middle-aged,” and the “old.” Our model enables a tractable quantitative analysis of optimal policy. For baseline parameter values for the COVID-19 pandemic applied to the US, we find that optimal policies differentially targeting risk/age groups significantly outperform optimal uniform policies and most of the gains can be realized by having stricter protective measures such as lockdowns on the more vulnerable, old group. Intuitively, a strict and long lockdown for the old both reduces infections and enables less strict lockdowns for the lower-risk groups. (JEL H51, I12, I18, J13, J14)*

The principle of targeting plays an important role in economic analyses of government policy. Applying this well-respected principle is another matter, one that requires showing substantial benefits on a case-by-case basis. In many epidemics, the risk of infection or serious health complications varies greatly between different demographic groups, and so does the cost of lockdowns and preventative actions. The COVID-19 pandemic, which has led to more than 4.5 million confirmed deaths worldwide (as of August 28, 2021) and led to the largest global recession of the last nine decades, is no exception. It is distinguished by a very steep mortality risk (case fatality rate) with respect to age: for those over 65 years of age, mortality from infection is about 60 times that of those aged 20–49. Differences of this magnitude merit examining the benefits of targeted policies.

In this paper we develop a multigroup version of the epidemiological SIR population-based model (Kermack and McKendrick 1927) and undertake a quantitative analysis of optimal policy in this framework. Focusing on a case with three groups

\*Acemoglu: MIT Economics Department (email: [daron@mit.edu](mailto:daron@mit.edu)); Chernozhukov: MIT Economics Department (email: [chernozhukov@gmail.com](mailto:chernozhukov@gmail.com)); Werning: MIT Economics Department (email: [iwerning@mit.edu](mailto:iwerning@mit.edu)); Whinston: MIT Economics Department and Sloan School of Management (email: [whinston@mit.edu](mailto:whinston@mit.edu)). Pete Klenow was coeditor for this article. Rebekah Anne Dix and Tishara Garg provided excellent research assistance. For useful conversations, comments, and suggestions we thank Fernando Alvarez, Alyssa Bilinski, Samantha Burn, Arup Chakraborty, Joe Doyle, Glenn Ellison, Zeke Emanuel, Ruth Faden, Eli Fenichel, Michael Greenstone, Simon Johnson, Angela McLean, Jessica Metcalf, Simon Mongey, Robert Shimer, and Alex Wolitzky, and especially three anonymous referees. We also thank Sang Seung Yi for providing us with the Korean case and mortality data. All remaining errors are our own.

<sup>†</sup>Go to <https://doi.org/10.1257/aeri.20200590> to visit the article page for additional materials and author disclosure statement(s).

(young, 20–49; middle-aged, 50–64; and old, 65+) and choosing parameters in line with the COVID-19 pandemic, we find that the benefits of targeting are significant.

When the options are restricted to uniform policies that treat all groups symmetrically, there are difficult trade-offs facing policymakers. When the priority is to save lives (a “safety-focused” approach), the economy will have to endure a lengthy lockdown and sizable declines in GDP. For example, to keep the mortality rate in the (adult, over 20) population below 0.1 percent, policymakers have to impose a full or partial lockdown of the economy for almost 1.5 years and put up with economic costs equivalent to as much as 25.9 percent of 1 year’s GDP. Conversely, an “economy-focused” approach attempting to keep economic damages to less than 10 percent of 1 year’s GDP would be forced to put up with a mortality rate of over 0.72 percent.

This policy trade-off can be significantly improved with targeted policies that employ differential lockdowns across groups, as the (“Pareto”) frontiers between economic damages and loss of life in Figure 1 illustrate. The dashed curve, representing the trade-off with targeted policies, is much closer to the “bliss point” (the origin) than is the solid frontier for uniform policies. For example, our quantitative analysis shows that, with the safety-focused objective, targeting can reduce economic damages from around 25.9 percent to about 17.6 percent.

We also show that, for our COVID-19-based parameters, almost all of the gains from targeting can be achieved without the need to resort to complicated targeting policies. Rather, a “semi-targeted” policy that simply treats the most vulnerable (older) age group differently than the rest of the population performs nearly as well as “fully targeted” policies (which also treat the young and middle-aged differentially). This is because it is optimal to impose a nontrivial lockdown on the young and middle-aged in order to protect the old who interact with others even under a strict lockdown, and the gains from full targeting are small relative to those of protecting the old from the younger groups’ network effects.

Three comments are useful at this point. First, throughout “lockdown” should be understood not simply as individuals staying home but as the suite of costly preventative actions (including social distancing) that reduce social and work interactions. Second, our focus is on optimal policies, and we return to the issue of implementation—how individuals can be encouraged to follow these policies and how much of it can take place voluntarily—only briefly at the end. It has to be borne in mind that government policies will change individual behavior in potentially complex ways, as some of the recent work endogenizing economic choices in models of epidemics has started recognizing.<sup>1</sup> Third, there is still much uncertainty about many of the key parameters for COVID-19 (Manski and Molinari 2020), and any optimal policy, whether uniform or not, will be highly sensitive to these parameters. Nonetheless, our general conclusion that targeted policies bring sizable benefits appears very robust.

Several recent papers independently investigate the role of age-dependent hospitalization and fatality rates in SIR models (Gollier 2020; Favero, Ichino, and Rustichini 2020; Rampini 2020; Bairoliya and İmrohoroğlu 2020; Brotherhood

<sup>1</sup> See Rowthorn and Toxvaerd (2020); Eichenbaum, Rebelo, and Trabandt (2020); Farboodi, Jarosch, and Shimer (2020); Jones, Philippon, and Venkateswaran (2020); Garibaldi, Moen, and Pissarides (2020); and Acemoglu et al. (forthcoming) as well as early related contributions such as Geoffard and Philippon (1996) and Fenichel (2013).

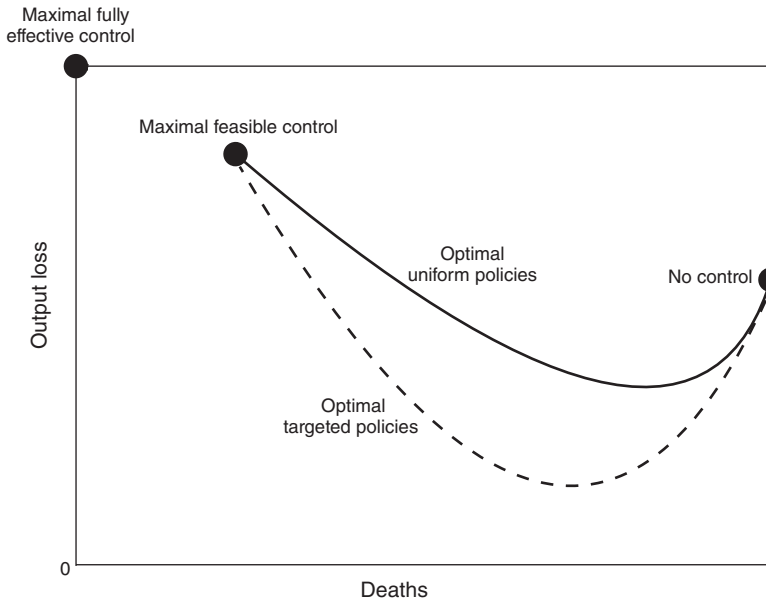


FIGURE 1. FRONTIER: ECONOMIC LOSSES VERSUS (EXCESS) DEATHS

et al. 2020; and Glover et al. 2020). The main difference is our systematic analysis of optimal policies. Brotherhood et al. (2020) and Glover et al. (2020) study infection and economic dynamics in settings with labor supply and consumption choices and present complementary results to ours, focusing on younger individuals' risk-taking behavior and the implications of this for testing and conditional quarantining or the conflict between the young and the old about mitigation policies, though Glover et al. (2020) also discuss optimal policy. Baqaee et al. (2020) present a model where policy is targeted according to age and sector to investigate alternative reopening scenarios (but consider only policies where policymakers link activity to the unemployment rate and whether deaths are high and/or rising).

The next section presents our multigroup SIR model. Section II describes our parameter choices. Our main results are presented in Section III, which also contains a number of robustness exercises. Section IV concludes.

## I. Multigroup SIR Model

### A. Model Assumptions

Time is continuous,  $t \in [0, \infty)$ , and individuals are partitioned into groups  $j = 1, \dots, J$  with  $N_j$  initial members. The total population is normalized to unity so that  $\sum_j N_j = 1$ . Individuals within each group are subdivided into susceptible (S), infected (I), recovered (R), and deceased (D),

$$S_j(t) + I_j(t) + R_j(t) + D_j(t) = N_j.$$

Agents move from susceptible to infected, then either recover or die. Groups interact within themselves as well as with each other, as described below.

Susceptible individuals become infected by coming into contact with infected individuals. Those who are infected may or may not require medical or intensive care unit (ICU) care. We suppose that the need for ICU care is immediately realized upon infection. Let  $\iota_j$  denote the constant fraction of infected people of type  $j$  needing ICU care. With Poisson arrival  $\delta_j^i$ , an ICU patient of type  $j$  recovers. Non-ICU patients do not die and recover with Poisson arrival  $\gamma_j$ . While in the ICU, patients die with Poisson arrival  $\delta_j^d(t)$ , depending on total ICU needs relative to capacity, where

$$\gamma_j = \delta_j^d(t) + \delta_j^r(t).$$

Let  $H_j(t)$  denote the number of type  $j$  individuals needing ICU care at time  $t$ , so that  $H_j(t) = \iota_j I_j(t)$ . We assume that the death probability conditional on ICU is a nondecreasing function of the total ICU needs,  $H(t) = \sum_j H_j(t)$ ,

$$\delta_j^d(t) = \psi_j(H(t)),$$

where  $\psi_j$  is nondecreasing.

Detection and isolation of infected individuals is imperfect. To avoid additional state variables, we assume that for each infected individual it is determined immediately upon infection whether detection and isolation are possible. We denote by  $\tau_j$  the constant probability that an infected individual of type  $j$  not needing ICU care becomes isolated. Similarly, we let  $\phi_j$  denote the probability that an individual of type  $j$  needing ICU care is isolated. Hence, the probability that an infected person fails to be isolated is

$$\eta_j \equiv 1 - (\iota_j \phi_j + (1 - \iota_j) \tau_j).$$

We assume that recovered agents are immune and do not become infected for the remaining duration of the pandemic.<sup>2</sup> However, due to imperfect testing, we suppose that only a fraction  $\kappa_j$  ( $\in [\iota_j \phi_j + (1 - \iota_j) \tau_j, 1]$ ) of recovered agents are identified and allowed to work freely. The remaining fraction is not identified and is subject to lockdowns.

A vaccine and a cure become available at some date  $T$  (see Acemoglu et al. 2020 for stochastic vaccine arrival).

## B. Lockdown Policies

As noted in the introduction, all policies reducing interpersonal interactions are referred to as “lockdown policies.” Individuals in group  $j$  produce  $w_j$  when they are not in lockdown and  $\xi_j w_j$  during lockdown, where  $\xi_j \in [0, 1]$  captures the relative productivity of home versus market production.

<sup>2</sup>At this time this hypothesis is not backed by conclusive evidence.

We denote by  $L_j(t) \in [0, 1]$  the extent of lockdown for group  $j$ . A full lockdown ( $L_j = 1$ ) creates a loss for each member of group  $j$  equal to  $(1 - \xi_j)w_j$ .<sup>3</sup> Full lockdown may not be feasible, however, because of essential industries, so we impose  $L_j(t) \leq \bar{L}_j \leq 1$ .<sup>4</sup>

Importantly, even if full lockdown were feasible, it would not eliminate all human interactions and contagion. Thus, we assume that lockdown  $L_j(t)$  reduces actual work by  $L_j(t)$  but decreases the presence of group  $j$  in infectious interactions only by a factor  $1 - \theta_j L_j(t)$ , where  $\theta_j \leq 1$ . This may be because people are still allowed on the streets and transmission occurs when they cross paths or because people disobey lockdowns. One implication of such imperfect lockdowns is that it is never feasible to completely isolate one of the groups (for example, the old), and our analysis recognizes this constraint.

### C. Dynamics in Multigroup SIR

Before the vaccine and cure, for  $t \in (0, T)$ , infections for group  $j$  evolve according to the differential equation

$$\dot{I}_j = \beta(1 - \theta_j L_j) S_j \sum_k \rho_{jk} \eta_k (1 - \theta_k L_k) I_k - \gamma_j I_j$$

for  $\beta > 0$  and contact coefficients  $\{\rho_{jk}\}$  that allow for different contact rates across groups.

This is the classic law of motion of SIR models, assuming a “quadratic matching technology,” whereby more people available for matching does not create any congestion.<sup>5</sup>

The rest of the laws of motion for  $t \in (0, T)$  are

$$\dot{S}_j = -\dot{I}_j - \gamma_j I_j,$$

$$\dot{D}_j = \delta_j^d(t) H_j,$$

$$\dot{R}_j = \delta_j^r(t) H_j + \gamma_j (I_j - H_j),$$

where, again,  $H_j = \iota_j I_j$  denotes the number of ICU patients in group  $j$ .

After the vaccine and cure arrive at  $T$ , every individual that is alive is placed in the recovered category:  $S(t) = I(t) = 0$  for  $t \geq T$ .

Our multigroup SIR model displays a useful aggregation property, behaving like a single-group SIR model in special cases when lockdowns are uniform. Suppose

<sup>3</sup> $w_j$  may also include nonmonetary costs of lockdowns as we discuss in Section IIIB.

<sup>4</sup>We assume that intermediate  $L_j(t)$  values select the individuals to be locked down randomly. Policies that lock down the same people persistently can be incorporated into our framework by splitting identical workers into different groups that can be treated differently.

<sup>5</sup>In Acemoglu et al. (2020), we considered a more general, nonquadratic model, where

$$M_j(S, I, R, L) \equiv \left( \sum_k \rho_{jk} [(S_k + \eta_k I_k + (1 - \kappa_k) R_k)(1 - \theta_j L_k) + \kappa_k R_k] \right)^{\alpha-2}$$

(with  $\alpha \in (0, 2]$ ) multiplies the right-hand side of this equation. We also showed how this matters for certain aspects of optimal policy against the pandemic but does not reduce the benefits of targeted policies.

that effective contact rates and resolution rates out of infection are the same across groups, so that  $\rho_{jk} = \rho$  and  $\gamma_j = \gamma$ , and consider uniform lockdown policies,  $L_j(t) = L(t)$  for all  $j$ . Suppose further that infection rates are initially identical across groups so that  $S_j(0)/N_j$ ,  $I_j(0)/N_j$ , and  $R_j(0)/N_j$  are independent of  $j$ . Then, despite differences in case fatality rates, the evolution of infections within each group, and hence aggregate infections, is identical to that of a single-group SIR model. The same is not true for deaths—these are different across groups but do not affect the evolution of infections. This aggregation result is verified in our simulations for uniform policies.

#### D. Optimal Policies

The planner controls lockdown for each group  $\{L_j(t)\}_j$  for all  $t \in [0, T]$ . Throughout, the planner will try to minimize a combination of total (excess) deaths during the pandemic, lives lost  $= \sum_j D_j(T)$ , and economic losses  $= \int_0^T \sum_j \Psi_j(t) dt$ , where

$$\begin{aligned} \Psi_j(t) = & (1 - \xi_j) w_j S_j(t) L_j(t) + (1 - \xi_j) w_j I_j(t) (1 - \eta_k (1 - L_j(t))) \\ & + (1 - \xi_j) w_j (1 - \kappa_j) R_j(t) L_j(t) + \Delta_j w_j L_j \delta_j^d(t) I_j(t) \end{aligned}$$

captures the economic losses from the lockdowns of susceptible individuals (first term), the isolation of some of the infected (second term), the lockdown of some of the recovered (third term), and the lost production of those who die (fourth term, in which  $\Delta_j w_j$  is the present discounted value of a group  $j$  member’s output until retirement lost due to death). Notice that we are incorporating the loss of future output from each death into the economic costs, but this is separate from the planner’s objective of minimizing lives lost (and in this latter objective, we do not distinguish lives by future economic losses).

Although the exact form of the optimal lockdown is complex, one can distinguish two broad strategies: the planner can “wait for the vaccine” (slowing down the spread of the virus to limit infections until the vaccine arrives) or alternatively go for “herd immunity.” In fact, there are many ways to reach herd immunity, and different policies can steer the pandemic toward different herd immunity outcomes.

To illustrate, suppose that there are two equal-sized groups, the old and the young, and  $\rho = \eta = 1$ . Figure 2 shows, for this case, the time path for the pair  $(S_y(t), S_o(t))$  over the course of the pandemic for  $t \in [0, T]$  until the arrival of the vaccine. The pandemic starts near  $(1, 1)$  with few infections and travels down and to the left as more people get infected.

The shaded area represents the region of herd immunity, where the size of the susceptible population is sufficiently low that, once we enter this region before  $T$ , the pandemic comes to an end quickly.<sup>6</sup> In single-group SIR models, this region

<sup>6</sup>More formally, we can define the region of herd immunity as the set of points  $(S_y, S_o)$  with the property that, in the absence of lockdowns  $L_y(t) = L_o(t) = 0$ , the dynamic system starting from  $(S_y(0), S_o(0)) = (S_y, S_o)$  and small initial infections  $(I_y(0), I_o(0))$  converges to points near  $(S_y, S_o)$ . In other words  $(S_y(\infty), S_o(\infty))$  is continuous in  $(I_y(0), I_o(0))$  so that for the limit point  $(S_y(\infty), S_o(\infty))$  we have  $(S_y(\infty), S_o(\infty)) \rightarrow (S_y, S_o)$  as  $(I_y(0), I_o(0)) \rightarrow (\bar{I}_y(0), \bar{I}_o(0))$ . One can express this property as a condition on the largest (dominant) eigenvalue of the linearized dynamical system.

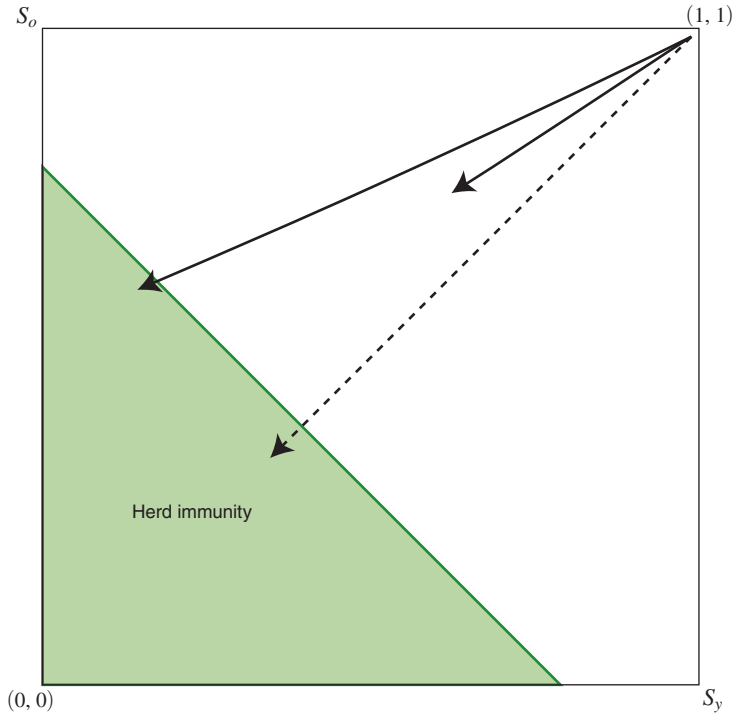


FIGURE 2. ILLUSTRATIVE HERD IMMUNITY REGION AND DIFFERENT TIME PATHS FOR THE PANDEMIC WITH TWO GROUPS, OLD AND YOUNG

corresponds to an interval of the form  $S \in [0, \bar{S}]$ , and within this interval we have  $\dot{I} < 0$ . With multiple groups, this same concept defines a region for the pair  $(S_y, S_o)$ . When  $\rho = \eta = 1$  and the two groups have equal sizes, this region is symmetric, with slope  $-1$ , as shown in the figure.

Without any mitigation, the disease follows the dashed 45-degree line, starting from an initial condition where almost nobody has been sick and reaching a situation where the majority in both groups have been infected at some point. The pandemic goes beyond the frontier for herd immunity—a phenomenon referred to as “overshooting”—because infections continue to spread for a while as there are many infected individuals when we cross the threshold. Although the pandemic travels along the 45-degree line so that the same fraction of young and old get infected, mortality will be significantly higher for the old given their higher case fatality rate.

Different lockdown policies induce different trajectories toward the herd immunity region: the ones that do not reach the herd immunity region before  $t = T$  are waiting for the vaccine, while those that reach this region before  $t = T$  are going for herd immunity.

Any uniform policy sends  $(S_y, S_o)$  along the 45-degree line by virtue of our aggregation result. More targeted mitigation policies open up new possibilities. The top solid line locks down the old more aggressively than the young, leading to lower infections among old relative to young. The resulting trajectory then reaches the region of herd immunity at an angle, with a higher fraction of infected among the young than the old, reducing excess mortality for the old. With targeted policies,

too, the planner may opt to hold out for the vaccine as with the lower solid line but can do so while reducing infections among the old.

## II. Specification and Calibration

We focus on targeting policies based on age with three groups, the “young” ( $y$ ), who are ages 20–49; the “middle-aged” ( $m$ ), who are 50–64; and the “old” ( $o$ ), who are 65 and older. We do not include those under 20 in our analysis.<sup>7</sup> We take the population share of these three groups among those over 20 years of age from the Bureau of Labor Statistics population data for 2019,  $N_y = 0.53$ ,  $N_m = 0.26$ , and  $N_o = 0.21$ . We assume equal earnings per capita for the young and middle-aged groups, which we normalize by setting  $w_y = w_m = 1$ , while  $w_o = 0.26$ .<sup>8</sup> We set  $\xi = 0.4$ , which implies that working from home results, on average, in a 60 percent loss of productivity, which matches Dingel and Neiman’s (2020) estimate that 37 percent to 46 percent of the US workforce can work from home.

As in Alvarez, Argente, and Lippi (2020), we set  $\bar{L} = 0.7$  when we consider uniform policies, reflecting the need for essential services by 30 percent of the workforce, and set  $\bar{L}_o = 1$  and  $\bar{L}_j = 0.7$  for the other groups when considering targeted policies. We set  $\phi_j = \tau_j = 0.1$ , implying that the probability of failing to isolate an infected individual is  $\eta_j \equiv \eta = 0.9$  for all groups. We also assume that there is perfect identification of individuals who have recovered and are allowed to go back to work, so that  $\kappa_j = 1$ .<sup>9</sup>

We choose  $\gamma = 1/18$  so that a COVID-19 case reaches a conclusion, with the individual either recovering or dying, in 18 days on average.<sup>10</sup> We set  $\beta$  equal to 0.106, which implies a reproduction rate of  $R_0 = 1.9$ . This choice is motivated by the baseline numbers in Ferguson et al. (2020), which gave a value of  $R_0 = 2.4$  for the beginning of the pandemic, combined with more recent evidence, which suggests that minimal precautions (such as basic sanitary measures and masks) have reduced transmissions by about 20 percent (Baqae et al. 2020; Chernozhukov, Kasha, and Schrimpf 2020).

We set  $\theta = 0.75$  in our baseline and examine lower values of  $\theta$  in our robustness analysis. This value of  $\theta$  implies that a full lockdown reduces interactions by 75 percent. For the contact matrix  $\{\rho_{ij}\}$ , we start with a conservative benchmark and assume  $\rho_{ij} = 1$  for all  $i, j$ , so that all age groups interact equally with each other. This is not meant to be realistic, but it enables transparency and diminishes

<sup>7</sup> Another factor that targeted policies could depend on is the presence of comorbidities, which have been shown to lead to significantly higher mortality and ICU needs. We focus on age in part because of the availability of mortality risk data by age group and the greater feasibility of implementing age-based policies.

<sup>8</sup> From Bureau of Labor Statistics statistics, the full-time employed middle-aged have 12 percent higher weekly earnings but are 13 percent less likely to be employed than the young. The share of workers who are employed full time versus part time is roughly equal in the two groups. Only 20 percent of those over 65 work and, when employed, earn slightly more, leading to  $w_o = 0.26$ . In Section IIIB, we also include utility costs from lockdown, which affect the relative opportunity costs of lockdown by group but do not change our overall qualitative and quantitative conclusions.

<sup>9</sup> In Acemoglu et al. (2020), we show that relaxing this assumption has no major effect on our results.

<sup>10</sup> Setting  $\gamma = 1/5$  or  $1/7$  to match the length of time during which an individual is infectious and then recalibrating  $\beta$  to match the same level of  $R_0$  leads to essentially identical results.



benefits from targeting, as the old will be more exposed to the infected among the younger groups.

We take from Ferguson et al. (2020) the case fatality rates for the three age groups, conditional on infection and ICU services being available as  $(\bar{\delta}_y^d = 0.001, \bar{\delta}_m^d = 0.01, \bar{\delta}_o^d = 0.06)$ . These numbers are in line with those from South Korea and the Diamond Princess cruise (see Acemoglu et al. 2020 for details and discussion). We also choose  $\iota_j = 0.0076 \bar{\delta}_j^d$  based on the fraction of infections requiring ICU care by age used in Ferguson et al. (2020), adjusted for the structure of the US population. We specify that base mortality rates are multiplied by a factor  $[1 + \lambda H(t)]$  and choose  $\lambda$  so that a 10 percent uniform infection rate increases mortality by 10 percent.

We set the present discounted value of the lost work life of the three groups upon death,  $(\Delta_y, \Delta_m, \Delta_o)$ , by assuming a retirement age of 67.5 years, so that there are 32.5 remaining work years for the young, 10 years for the middle-aged, and 2.5 years for the old. We also set the interest rate at 1 percent.

Finally, in our baseline we have  $T = 546$  days, corresponding to vaccine arrival in 1.5 years time, and set initial conditions for each group as 99 percent susceptible, 0.5 percent infected, and 0.5 percent recovered.

To generate our frontiers, we minimize  $\int_0^T \sum_j \Psi_j(t) dt + \chi \sum_j D_j(T)$ , that is, the sum of economic damages and  $\chi$  times the number of deaths, subject to the laws of motion of our model; we then vary the parameter for the nonpecuniary cost of life,  $\tilde{\chi}$ . We use a discrete-time approximation to this optimal control problem and then apply a nonlinear interior point algorithm to compute the solutions (Wächter and Biegler 2006). We utilize the APMonitor-Gekko interface to implement the interior point algorithm (Hedengren et al. 2014, Beal et al. 2018). The numerical solutions are not sensitive to initial conditions.

### III. Optimal Policies

#### A. Main Results

Figure 3 depicts the frontier between lives lost and economic damages under different policies for our baseline parameters and summarizes the trade-off faced by policymakers. As in Figure 1 in the introduction, the bliss point is the origin, where there are no (excess) lives lost and no economic damages. Each curve in the figure represents the frontier resulting from a different class of policies: the top (red) frontier is for uniform policies. Below it we have the (green) frontier for semi-targeted policies, which set the same lockdown policy for the young and the middle-aged and a different policy for the 65+ group. Slightly below this (in blue) is the frontier for fully targeted policies. The convex shape of the frontiers represents diminishing returns to pursuing one objective at the expense of the other.

The trade-off facing policymakers when the menu of options is limited to uniform policies is grim. For example, policymakers prioritizing saving lives could aim to keep total mortality from COVID-19 to less than 0.1 percent of the (adult) population. This safety-focused optimal uniform policy, depicted in the top left panel of Figure 4, involves a (partial) lockdown until the vaccine's

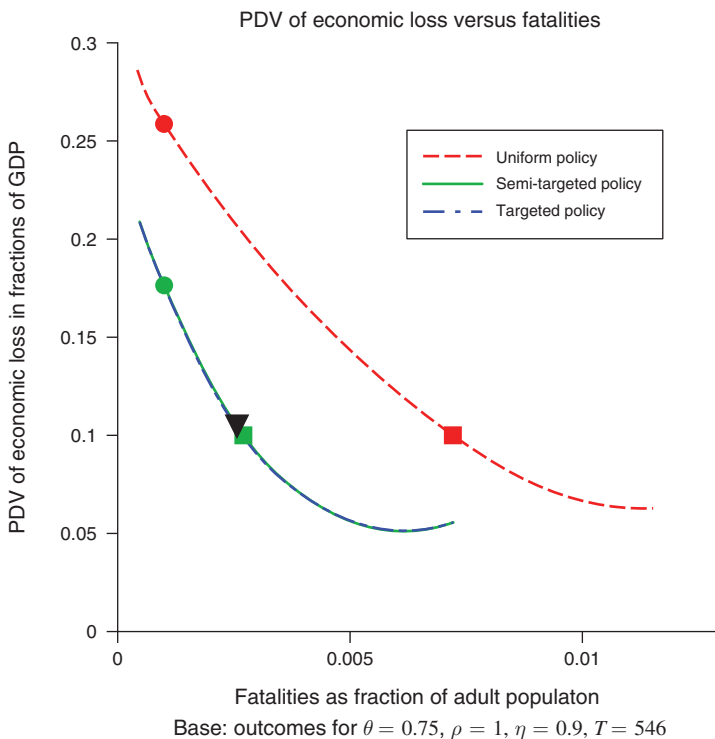


FIGURE 3. FRONTIERS OF OUTPUT LOSS VERSUS DEATHS FOR BASELINE SPECIFICATION

Notes: The three frontiers represent different levels of targeting. The circles show the safety-focused policies, the squares are for the economy-focused policies, and the triangle depicts the optimal semi-targeted policy for a nonpecuniary cost of death  $\chi = 35$ , which supports the safety-focused optimal uniform policy.

arrival.<sup>11</sup> This lengthy lockdown has significant economic costs, amounting to 25.9 percent of 1 year’s GDP (25.35 percent of this damage is in terms of economic losses during the 1.5 year duration of the pandemic, and the remaining 0.55 percent is due to forgone productive contributions from excess deaths). Consistent with our aggregation result, the infection rates for the three age groups are on top of each other in the top right panel of Figure 4. Nevertheless, the table in the top right corner of the figure shows that mortality rates are much higher for the older group, reflecting their higher case fatality rate. The time path of the infection rate follows an inverse U-shape, typical in SIR models, peaking in about 1.5 months and declining slowly thereafter. The behavior of the infection rate also reveals that optimal policy in this case is waiting for the vaccine: when the lockdown is lifted shortly before the vaccine’s arrival, there is no herd immunity and the infection rate starts increasing immediately (only to be brought under control by the vaccine).<sup>12</sup>

<sup>11</sup> This policy would be optimal, alternatively, if we set  $\chi = 35$ , which translates into a value of statistical life of \$3.8 million for an average young person or an average value of life year of about \$286,000 in the population (in both cases inclusive of the economic and nonpecuniary costs). See Acemoglu et al. (2020) for details.

<sup>12</sup> Safety-focused optimal uniform policy yields a mortality rate of 0.0053 percent for the adult population and thus total deaths of about 175,500 by the ninth month of the pandemic, compared to about 320,000 deaths in the United States by the end of December 2020.

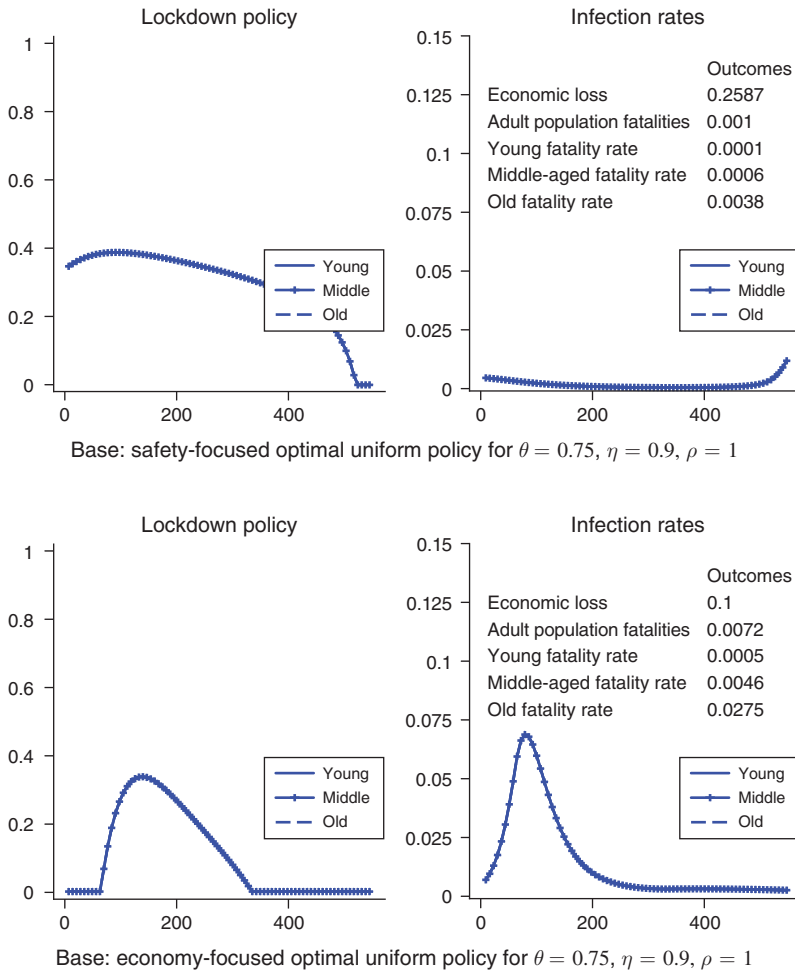


FIGURE 4

Note: Optimal uniform policy for baseline parameters that achieves the “safety-focused” objective of limiting the population mortality rate to no more than 0.1 percent (top two panels) and the “economy-focused” objective of limiting economic losses to no more than 10 percent of 1 year’s GDP (bottom two panels).

The economy-focused optimal uniform policy, limiting economic damages to no more than 10 percent of 1 year’s GDP, is shown in the bottom panel of Figure 4.<sup>13</sup> In this case, a significantly higher fraction of the population, about 0.7 percent, will perish because of the disease. Differently from the safety-focused optimal uniform policy, the economy-focused policy goes for herd immunity, with a shorter lockdown aimed at flattening the curve of the infection and avoiding overwhelming ICU capacity. Infections now peak at a higher level, about 7 percent, but they also decline to zero and never show a further uptick.

Our main result can be gleaned by comparing the uniform and semi-targeted frontiers in Figure 3. For the safety-focused objective, which aims to keep total mortality

<sup>13</sup>The value of a life for an average young person that would justify the economy-focused policy, corresponding to  $\tilde{\chi} = 18.6$ , is \$2.8 million, compared to \$3.8 million for the safety-focused policy.

from the virus to less than 0.1 percent, a semi-targeted policy can reduce economic losses from the 25.9 percent mentioned to about 17.6 percent (16.8 percent of this coming in the form of a decline in current GDP). The form of the safety-focused semi-targeted optimal policy is depicted in the top panel of Figure 5. The lockdown is very strict on the older group and much less strict on the rest of the population. The safety-focused optimal semi-targeted policy also waits for the vaccine for the older group (who are in lockdown until the vaccine's arrival) but only partially so for the rest of the population (whose curve is again flattened so much that by the time the vaccine arrives, there is still no population-wide herd immunity, as can be seen from the uptick of the infections just before the vaccine). Finally, the infection rate of the 65+ group reaches a smaller peak than under uniform policies, because they are protected by their more strict lockdown. Notably, however, they are still being infected by the young and the middle-aged because  $\theta = 0.75$  implies that they are in not-too-infrequent contact with these younger groups, which is exactly the reason why the optimal semi-targeted policy keeps the young and the middle-aged under a relatively long lockdown.

The middle panel of Figure 5 turns to the economy-focused optimal semi-targeted policy and shows that now the adult mortality rate is 0.27 percent, rather than 0.72 percent under the economy-focused optimal uniform policy. The economy-focused optimal policy is still going for herd immunity but with a nuance: herd immunity is achieved primarily with the infections of the young and the middle-aged, while the more vulnerable older group is protected. Herd immunity also explains why the older group is allowed to come out of lockdown gradually starting in about a year.

Finally, the bottom panel of Figure 5 shows the optimal semi-targeted policy when we use the same value of the parameter for nonpecuniary value of life,  $\chi = 35$ , that supports the safety-focused uniform policy. Semi-targeted policies at this level of  $\chi$  encourage the social planner to exploit the gains from targeting in terms of improved economic performance, leading to economic damages of only 12.8 percent.<sup>14</sup>

A surprising result is that fully targeted policies that treat the young and the middle-aged differently perform essentially as well as semi-targeted policies. Indeed, in Figure 3 the blue fully targeted frontier is nearly indistinguishable from the green semi-targeted frontier. Figure A1 in the online Appendix verifies that the middle-aged, who have higher mortality rates from the virus than the young, are put under a stricter and longer lockdown. This improves outcomes, but only by a minuscule amount. The reason is that, as noted above, the main objective of locking down the under-65 groups is to protect the most vulnerable, 65+, group, and the comparatively small differences between the middle-aged and the young do not contribute much to the gains.

Figure A2 in the online Appendix shows that the differential lockdowns on the old are mostly because of their higher vulnerability, not because of their lower market wage. There, we distinguish between old-retired and old-workers and assume that the old-workers have the same wage as the middle-aged and the young but the same vulnerability to the virus as the old-retired. The optimal policy treats them very similarly to the old-retired. For example, in the safety-focused semi-targeted policies, they are put under lockdown until the vaccine arrives.

<sup>14</sup>When we consider the social planner's choice for a fixed  $\chi$ , it is not uncommon to see improvements only in one dimension, as targeting alters the trade-off between economic damages and fatalities. In particular, fatalities for a fixed  $\chi$  may rise when the slope of the frontier with targeted policies is steeper at the same level of fatalities.

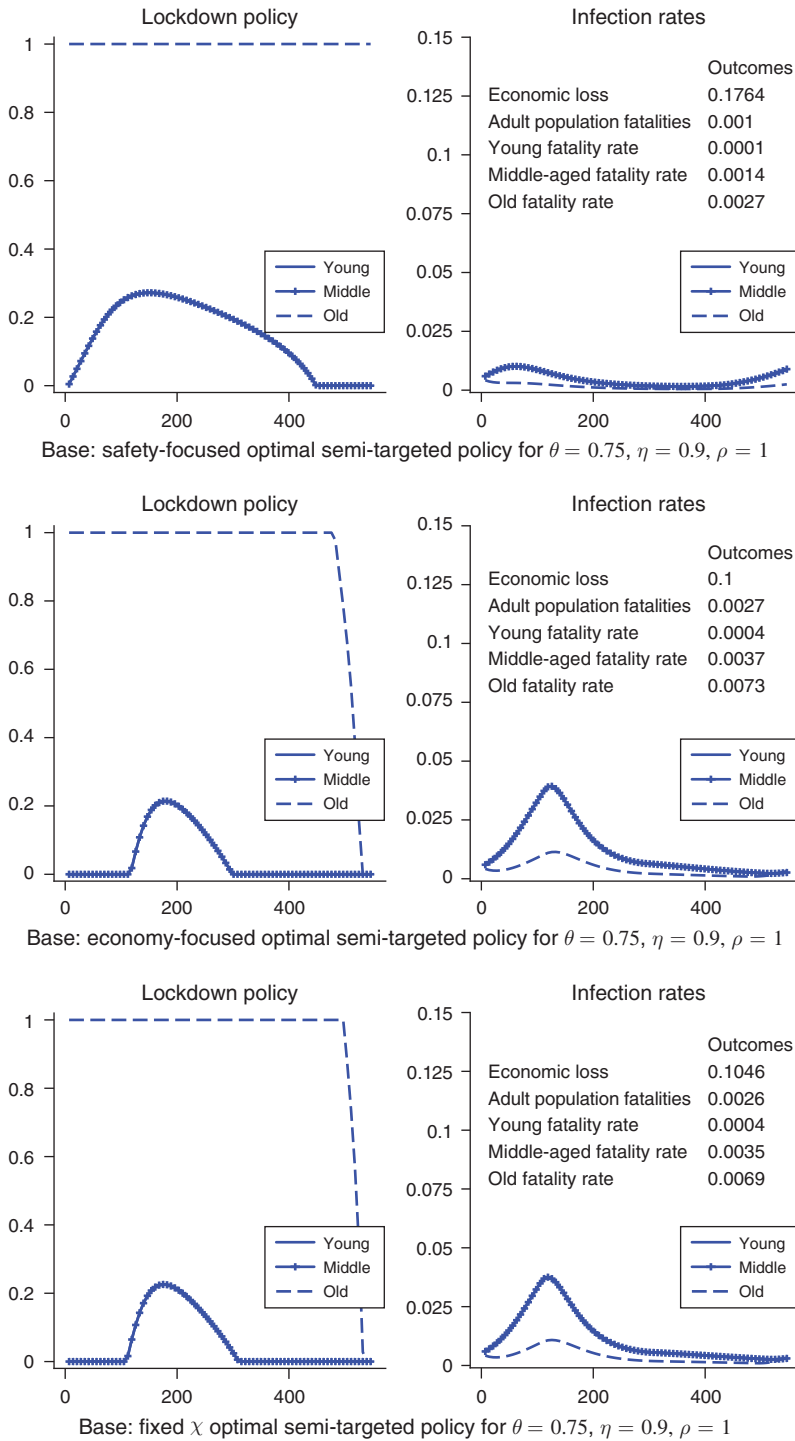


FIGURE 5

Note: This figure displays “safety-focused” semi-targeted optimal policy (top two panels); “economy-focused” semi-targeted optimal policy (middle two panels); and optimal semi-targeted policy with nonpecuniary cost of death  $\chi = 35$  (bottom two panels).

Overall, our results establish that targeted policies can significantly improve the trade-offs between lives lost and economic damages from the pandemic, and most of the gains can be achieved with simple semi-targeted policies that apply more strict lockdowns on the oldest, most vulnerable group.

### B. Robustness

We explored the robustness of these results in a number of directions. In all cases, the significant gains from semi-targeting and the small additional benefits from full targeting remain. The details of these robustness exercises are provided in Acemoglu et al. (2020). Here we discuss five that are particularly important. First, many works in the epidemiology literature impose a hard constraint on ICU capacity (because they view overrunning ICU capacity as extremely costly) and consider simple lockdown policies, often showing a pattern in which lockdowns are lifted and then reimposed, leading to several waves. When we impose such a hard constraint (equal to 115 percent of the pre-COVID ICU capacity of about 32,000), we find that this pattern of on and off policies is not optimal, and targeted lockdowns lead to benefits similar to those shown above, despite the hard constraints. Online Appendix Figure A3 illustrates this point for optimal policies targeting 15 percent economic losses in the uniform policy and targeting 10 percent economic losses in the semi-targeted policy.<sup>15</sup> Second, we show in online Appendix Figure A4 that the results are very similar when we use the value of  $\beta$  implied by the original numbers in Ferguson et al. (2020).<sup>16</sup> Third, we introduce an additional utility cost from lockdowns for all groups equal to 30 percent of the young and the middle-aged wage, which implies that the opportunity cost of lockdowns for the old is higher than in our baseline. Nevertheless, online Appendix Figure A5 shows that the gains from targeting and the form of optimal semi-targeted policies remain very similar. Fourth, we depart from the quadratic matching technology and show that this also has no major effect on our conclusions (though the formal matching technology does matter for other aspects of policy). Finally, we extend our analysis to the more realistic SEIR model (involving exposed, E, individuals). This has essentially no effect on our conclusions; see online Appendix Figure A6 and Acemoglu et al. (2020).

### C. Network Structure, Group Distancing, and Testing

Introducing differential social interactions between different groups (relaxing the assumption that  $\rho_{jk} = 1$ ) is not only useful for realism but also enables us to consider a richer set of policies, such as group distancing ones aimed at reducing between-group transmissions. Here we use data from Klepac et al. (2020), based on the BBC pandemic project, for interaction patterns across different age groups in

<sup>15</sup>The uniform economy-focused policy targeting 10 percent loss is not feasible with the ICU capacity constraint imposed, and therefore we used 15 percent loss as the target to illustrate the shape of the optimal lockdown profiles and infection rates. On the other hand, in the semi-targeted policy, it is possible to maintain 10 percent economic loss without the ICU capacity constraint binding, so the result is exactly the same as without the ICU capacity constraint.

<sup>16</sup>This was the baseline in the working paper version of our work, Acemoglu et al. (2020).

the United Kingdom, which suggest moderately higher within-group contact rates. Online Appendix Figures A7 and A8 show that optimal semi-targeted lockdowns (with the baseline SIR model and the SEIR extension, respectively) again bring significant gains and are on the whole similar to those shown here—except that there is now some relaxation of lockdowns on the 65+ group to take advantage of the lower interactions between this group and other, higher-infection groups, followed by a subsequent retightening. Next, we also introduce testing policies that help isolate infected individuals at a higher rate. Group distancing and testing policies, either by themselves or combined, make targeted policies even more powerful. For example, if the two are combined, optimal semi-targeted policies are enough to keep infections very low and the overall mortality rate at 0.1 percent at an economic cost of just 4.8 percent of GDP (see online Appendix Figure A9 and Acemoglu et al. 2020 for more details).

#### IV. Conclusions

We developed a framework for optimal policy analysis in a multigroup SIR model. Our analysis shows that simple but ad hoc policies may sometimes lead to highly suboptimal performance, and especially in the case of the COVID-19 pandemic, age-targeted policies can significantly improve economic and public health outcomes. Our quantitative conclusions are quite consistent across different parameterizations and are the main take-away message from the paper.

We did not consider how optimal policies can be implemented, which is important for at least two reasons. First, voluntary behavioral changes may already achieve some, but typically not all, of the objectives of optimal policy, and it is important to investigate the form and extent of government lockdown requirements in the presence of behavioral adjustments and whether they need to be differential across groups (or whether uniform requirements may sometimes lead to optimally differential behavior). Second, in the presence of voluntary social distancing, government policies may sometimes backfire. For example, Acemoglu et al. (forthcoming) show that testing policies may generate excessive slackening of voluntary social distancing, especially among high-risk groups. These two considerations together imply that there could be a type of “Lucas critique” when it comes to mitigation policies: once lockdown or testing policies are changed, the law of motion of the pandemic responds. This obviously calls for the study of more micro-founded models of individual behavior in the course of a pandemic.

#### REFERENCES

- Acemoglu, Daron, Victor Chernozhukov, Iván Werning, and Michael D. Whinston. 2020. “A Multi-Risk SIR Model with Optimally Targeted Lockdown.” NBER Working Paper 27102.
- Acemoglu, Daron, Victor Chernozhukov, Iván Werning, and Michael D. Whinston. 2021. “Replication Data for: Optimal Targeted Lockdowns in a Multigroup SIR Model.” American Economic Association [publisher], Inter-university Consortium for Political and Social Research [distributor]. <https://doi.org/10.3886/E130626V1>.
- Acemoglu, Daron, Ali Makhdomi, Azarakhsh Malekian, and Asuman Ozdaglar. Forthcoming. “Testing, Voluntary Social Distancing and the Spread of an Infection.” *Operations Research*.
- Alvarez, Fernando E., David Argente, and Francesco Lippi. 2020. “A Simple Planning Problem for COVID-19 Lockdown.” NBER Working Paper 26981.

- Bairoliya, N., and A. İmrohoroğlu.** 2020. "Macroeconomic Consequences of Stay-At-Home Policies during the COVID-19 Pandemic." Unpublished.
- Baqace, David, Emmanuel Farhi, Michael J. Mina, and James H. Stock.** 2020. "Reopening Scenarios." NBER Working Paper 27244.
- Beal, Logan D.R., Daniel C. Hill, R. Abraham Martin, and John D. Hedengren.** 2018. "GEKKO Optimization Suite." *Processes* 6 (8): 106.
- Brotherhood, Luiz, Philipp Kircher, Cezar Santos, and Michèle Tertilt.** 2020. "An Economic Model of the COVID-19 Epidemic: The Importance of Testing and Age-Specific Policies." IZA Discussion Paper 13265.
- Chernozhukov, Victor, Hiroyuki Kasaha, and Paul Schrimpf.** 2020. "Causal Impact of Masks, Policies, Behavior on Early COVID-19 Pandemic in the US." *Journal of Econometrics* 220 (1): 23–62.
- Dingel, Jonathan I., and Brent Neiman.** 2020. "How Many Jobs Can Be Done at Home?" NBER Working Paper 26948.
- Eichenbaum, Martin S., Sergio Rebelo, and Mathias Trabandt.** 2020. "The Macroeconomics of Epidemics." NBER Working Paper 26882.
- Farboodi, Maryam, Gregor Jarosch, and Robert Shimer.** 2020. "Internal and External Effects of Social Distancing in a Pandemic." NBER Working Paper 27059.
- Favero, Carlo A., Andrea Ichino, and Aldo Rustichini.** 2020. "Restarting the Economy While Saving Lives under COVID-19." CEPR Discussion Paper 14664.
- Fenichel, Eli P.** 2013. "Economic Considerations for Social Distancing and Behavioral Based Policies during an Epidemic." *Journal of Health Economics* 32 (2): 440–51.
- Ferguson, Neil M., Daniel Laydon, Gemma Nedjati-Gilani, Natsuko Imai, Kylie Ainslie, Marc Baguelin, Sangeeta Bhatia et al.** 2020. "Impact of Non-pharmaceutical Interventions (NPIs) to Reduce COVID-19 Mortality and Healthcare Demand." <https://doi.org/10.25561/77482>.
- Garibaldi, Pietro, Espen R. Moen, and Christopher A. Pissarides.** 2020. "Modelling Contacts and Transitions in the SIR Epidemics Model." *Covid Economics* 5: 1–20.
- Geoffard, Pierre-Yves, and Tomas Philipson.** 1996. "Rational Epidemics and Their Public Control." *International Economic Review* 37 (3): 603–24.
- Glover, Andrew, Jonathan Heathcote, Dirk Krueger, and José-Víctor Ríos-Rull.** 2020. "Health versus Wealth: On the Distributional Effects of Controlling a Pandemic." NBER Working Paper 27046.
- Gollier, Christian.** 2020. "Cost-Benefit Analysis of Age-Specific Deconfinement Strategies." <https://perso.math.univ-toulouse.fr/cattiaux/files/2020/04/gollier-22-04-2020slides.pdf>.
- Hedengren, John D., Reza Asgharzadeh Shishavan, Kody M. Powell, and Thomas F. Edgar.** 2014. "Nonlinear Modeling, Estimation and Predictive Control in APMonitor." *Computers & Chemical Engineering* 70: 133–48.
- Jones, Callum J., Thomas Philippon, and Venky Venkateswaran.** 2020. "Optimal Mitigation Policies in a Pandemic: Social Distancing and Working from Home." NBER Working Paper 26984.
- Kermack, William Ogilvy, and A. G. McKendrick.** 1927. "A Contribution to the Mathematical Theory of Epidemics." *Proceedings of the Royal Society A: Mathematical, Physical and Engineering Sciences* 115 (772): 700–721.
- Klepac, Petra, Adam J. Kucharski, Andrew J.K. Conlan, Stephen Kissler, Maria L. Tang, Hannah Fry, and Julia R. Gog.** 2020. "Contacts in Context: Large-Scale Setting-Specific Social Mixing Matrices from the BBC Pandemic Project." <https://doi.org/10.1101/111/2020.02.16.20023754>.
- Manski, Charles F., and Francesca Molinari.** 2020. "Estimating the COVID-19 Infection Rate: Anatomy of an Inference Problem." NBER Working Paper 27023.
- Rampini, Adriano A.** 2020. "Sequential Lifting of COVID-19 Interventions with Population Heterogeneity." NBER Working Paper 27063.
- Rowthorn, Robert, and Flavio Toxvaerd.** 2020. "The Optimal Control of Infectious Diseases via Prevention and Treatment." Cambridge-INET Working Paper Series 2020/13.
- Wächter, Andreas, and Lorenz T. Biegler.** 2006. "On the Implementation of an Interior-Point Filter Line-Search Algorithm for Large-Scale Nonlinear Programming." *Mathematical Programming* 106: 25–57.